Acta Biomaterialia 127 (2021) 193–204

Contents lists available at ScienceDirect

Acta Biomaterialia

journal homepage: www.elsevier.com/locate/actbio

Full length article

Tear propagation in vaginal tissue under inflation

Jeffrey A. McGuire[a], Jose L. Monclova[a], Adriana C. Salazar Coariti[b], Caleb A. Stine[c], Kimani C. Toussaint Jr.[b], Jennifer M. Munson[c], David A. Dillard[c], Raffaella De Vita[a,*]

[a] STRETCH Lab, Department of Biomedical Engineering and Mechanics, Virginia Tech, Blacksburg, VA 24061, United States
[b] PROBE Lab, School of Engineering, Brown University, Providence, RI 02912, United States
[c] Department of Biomedical Engineering and Mechanics, Virginia Tech, Blacksburg, VA 24061, United States

ARTICLE INFO

Article history:
Received 22 October 2020
Revised 6 March 2021
Accepted 30 March 2021
Available online 6 April 2021

Keywords:
Maternal trauma
Vaginal tissue
Inflation
Tear propagation
Digital image correlation
Second-harmonic generation imaging

ABSTRACT

Vaginal tearing at childbirth is extremely common yet understudied despite the long-term serious consequences on women's health. The mechanisms of vaginal tearing remain unknown, and their knowledge could lead to the development of transformative prevention and treatment techniques for maternal injury. In this study, whole rat vaginas with pre-imposed elliptical tears oriented along the axial direction of the organs were pressurized using a custom-built inflation setup, producing large tear propagation. Large deformations of tears through propagation were analyzed, and nonlinear strains around tears were calculated using the digital image correlation technique. Second harmonic generation microscopy was used to examine collagen fiber organization in mechanically untested and tested vaginal specimens. Tears became increasingly circular under pressure, propagating slowly up to the maximum pressure and then more rapidly. Hoop strains were significantly larger than axial strains and displayed a region- and orientation-dependent response with tear propagation. Imaging revealed initially disorganized collagen fibers that aligned along the axial direction with increasing pressure. Fibers in the near-regions of tear tips aligned toward the hoop direction, hampering tear propagation. Changes in tear geometry, regional strains, and fiber orientation revealed the inherent toughening mechanisms of the vaginal tissue.

Statement of significance

Women's reproductive health has historically been understudied despite alarming maternal injury and mortality rates in the world. Maternal injury and disability can be reduced by advancing our limited understanding of the large deformations experienced by women's reproductive organs. This manuscript presents, for the first time, the mechanics of tear propagation in vaginal tissue and changes to the underlying collagen microstructure near to and far from the tear. A novel inflation setup capable of maintaining the in vivo tubular geometry of the vagina while propagating a pre-imposed tear was developed. Toughening mechanisms of the vagina to propagation were examined through measurements of tear geometry, strain distributions, and reorientation of collagen fibers. This research draws from current advances in the engineering science and mechanics fields with the goal of improving maternal health care.

1. Introduction

Tearing of the vagina and surrounding structures is an all too familiar traumatic event associated with childbirth. More than 80% of women experience some degree of tissue laceration during their first vaginal deliveries [1,2]. The majority of these tears occur in the distal third of the vagina and they typically present in the sagittal plane [3,4]. These tears, commonly referred to as perineal tears, lead to obstetric anal sphincter injuries and, ultimately, to the onset of fecal incontinence [5]. More recently, data from prospective studies have captured the incidence of high vaginal tears. These tears occur within the upper two-thirds of the vagina [6] and usually present along the length of the vagina [4,7]. As much as 17% of women experience laceration of the vaginal tissue during delivery [8], and approximately 5% have vaginal tears without any perineal tearing [9]. Tears to the lateral walls of the vagina are considered clinical markers for levator ani avulsion [8], an established risk factor for pelvic organ prolapse [10]. The observed variation in

* Corresponding author.
E-mail address: devita@vt.edu (R. De Vita).

https://doi.org/10.1016/j.actbio.2021.03.065
1742-7061/

tearing by anatomical regions has been correlated with obstetric risk factors such as baby weight, operative delivery, and duration of the second stage of labor [9], but the cause of the variation is unknown, and it likely depends on the structure and mechanical properties of the vagina.

The vagina is a fibromuscular tubular organ with decreasing width and increasing thickness along its length from the proximal end to the distal end [11–14]. Through its thickness, the vagina is made of four main layers primarily composed of collagen, smooth muscle, and some elastin [15]. Histomechanical studies examined the regional variations and relationships between the microstructure and the uniaxial tensile response in the ewe vagina. It was found that collagen content was greatest toward the proximal end (near the cervix) relative to the distal end (near the introitus), corresponding to a stronger and stiffer tissue response at the proximal end [13,16]. In another study by Ulrich et al. [17], the authors revealed differences, although not significant, in collagen content and tangent modulus between the ventral (side closest to the urethra) and dorsal (side closest to the rectum) regions of the ovine vagina. However, significant differences in permanent strain between the ventral and dorsal ovine vaginas were observed.

While uniaxial tests provide basic mechanical properties such as tissue strength and tangent modulus in one loading direction, biaxial tests are physiologically more relevant and capture the complex loading conditions experienced by the vagina in vivo. By performing planar biaxial tests, Huntington et al. [18] and McGuire et al. [19] investigated the nonlinear anisotropic nature of the rat and swine vaginas, respectively. In their study, McGuire et al. [19] also studied the influence of pre-imposed tears and reported that, under sub-failure loads, the stress-stretch response of vaginal tissue was insensitive to tears. Moreover, they found that tears oriented in the hoop direction blunted significantly more than tears oriented in the axial direction. Similar to the planar biaxial tests, inflation tests by Robison et al. [20] and Clark et al. [14] on mice and McGuire et al. [21] on rats revealed the nonlinear anisotropy of the vagina. By conducting inflation tests up to rupture, McGuire et al. [21] discovered that tearing always presented within the mid-region of the rat vagina along the axial direction, with the vagina experiencing significantly larger hoop strains than axial strains.

Tearing of soft tissues has previously been examined via uniaxial notch tests [22–28] and biaxial notch tests [26,28,29]. Uniaxial studies on tendons and ligaments [23,24] as well as skin [25] and biaxial studies on amnion [26] and glisson's capsule [28] reported significant blunting of the notches without propagation of tears. Similarly, a study on knee meniscus [27] reported that the effective strength of the tissue was insensitive to the pre-imposed notch. These results have been attributed to collagen fiber straightening, sliding, and reorientation that serve to create a barrier to tear propagation in the near-field of notch tips. They have also been confirmed by small-angle X-ray scattering [25] as well as second-harmonic generation (SHG) imaging [26,28]. Significant strain concentrations at the notch tips have been reported together with the large degree of blunting [22,24,27]. This not only agrees with the large degree of blunting observed, but also suggests that significant shear strains may serve to redistribute the loads around the notch tip [24]. Interestingly, Haslach et al. [29] reported shear strain as a major contribution for through-thickness crack propagation of bovine aortas subjected to ring inflation tests.

With the exception of Haslach et al. [29], tearing in the above cited studies was investigated using either strips or sheets of tissues. The tear propagation in soft tissues with a more complex geometry and loading condition has never been investigated. The vagina has a tubular structure and can be viewed, to some extent, as a thin-walled cylindrical pressured vessel, experiencing significantly different stresses/strains in the hoop and axial directions. Thus tears are expected to propagate differently in such a configuration. Moreover, very little is known about the role of collagen fibers in vaginal tissue mechanics, so whether or not the toughening mechanisms against tear propagation are governed by the reorganization of collagen fibers remains unknown.

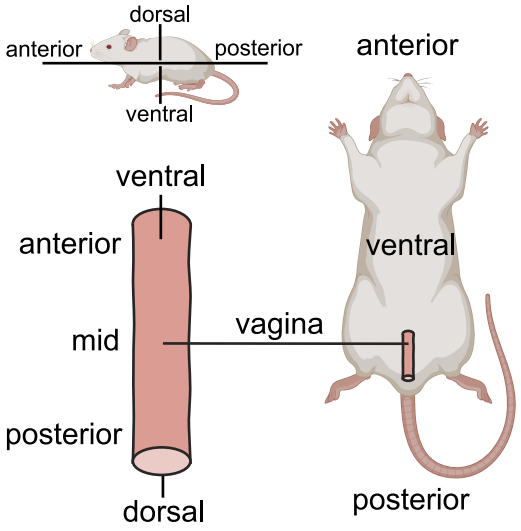

Fig. 1. Schematic of the anatomical regions of the rat vagina.

We hypothesize that the vaginal tissue, even with pre-imposed tears, will undergo large deformations when subjected to intraluminal pressure. We further hypothesize that the strains would be significantly different in the axial and hoop directions and highly inhomogeneous around the pre-imposed tears. Finally, we hypothesize that the collagen fibers within the vagina will re-organize to prevent tear propagation. To test our hypotheses, we designed and built an inflation testing setup that preserved the in vivo tubular structure of the rat vagina. We subjected whole rat vaginas with pre-imposed tears to intraluminal pressure and measured the resulting strains around the tear as well as the geometrical changes of the tear. Furthermore, we analyzed the local alterations in the collagen fiber morphology of the rat vagina that were induced by intraluminal pressure. Collectively, the findings of this study will advance our understanding of tear propagation in the vaginal wall.

2. Experimental methods

2.1. Specimen preparation

The current study was conducted with the approval of the Institutional Animal Care and Use Committee at Virginia Tech. Thirteen three-month-old, virgin female Sprague Dawley rats were sacrificed by decapitation, frozen at 20 °C and allowed to thaw at 4 °C before entire vaginas were isolated. The tissue specimens ($n = 13$) consisting of entire vaginas were hydrated with PBS, wrapped in gauze and frozen at 20 °C until inflation testing or imaging via multiphoton microscopy. Prior to inflation testing, a subset ($n = 10$) of the tissue specimens were thawed in PBS for 10 min and placed on a 6-gauge stainless steel dispensing needle for handling. While keeping the tissue specimens on the needles, cross-sectional images of the anterior (closer to the cervix, Fig. 1) ends were taken using a CMOS camera (DCC1645C, Thorlabs Inc., Newton, NJ) on a dissection microscope and measurements of the inner radius, R, and thickness, T, were performed from these images using ImageJ (NIH, Bethesda, MD). On average, the inner radius was 2.58 ± 0.03 mm and the thickness was 0.41 ± 0.05 mm. Cross-sectional images of the posterior (closer to the introitus, Fig. 1(a)) ends were not taken as these were generally thick containing bits

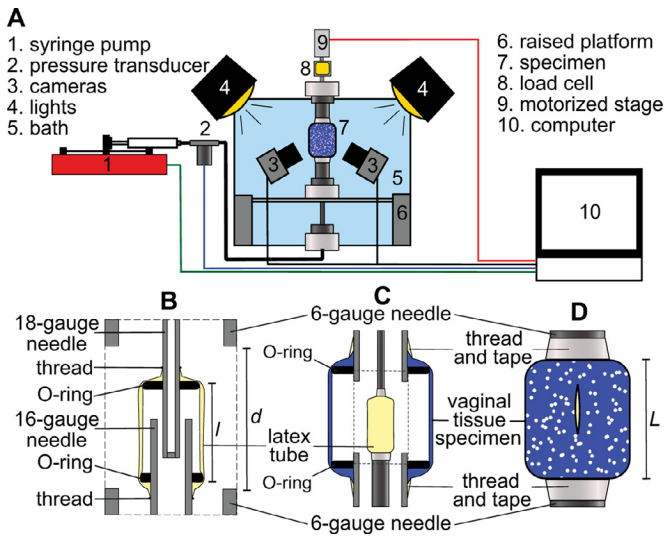

Fig. 2. (a) Schematic of the custom-made inflation setup for studying the tear propagation in rat vaginal tissue specimens. (b) Transverse cross-section of the latex tube mounted on two opposite coaxial (18-gauge and 16-gauge) needles. (c) Transverse cross-section of the vaginal tissue specimen mounted onto two opposite (6-gauge) needles over the latex tube. (d) Vaginal tissue specimen mounted over the latex tube and speckled for non-contact strain measurements. *l*: axial length of the latex tube, *L*: axial length of the vaginal tissue specimen, *d*: axial distance between the 6-gauge needles.

of extraneous tissue. An initial through-thickness tear along the axial direction was placed into the mid-region of the dorsal side of the tissue specimens (Fig. 1(a)) by first piercing the tissue specimens with an X-acto blade (#11, Elmer's Products Inc., Westerville, OH) then cutting using dissection microscissors (WPI Inc., Sarasota, FL). The size and orientation of the pre-imposed tear were selected based on the results of our previous study, where the average length of the tear was approximately 3 mm and tearing always occurred along the axial direction [21]. Here, the average initial length of the tears was 3.1 ± 0.2 mm.

2.2. Inflation setup

In order to study tear propagation of vaginal tissue specimens under inflation, an inflation setup was custom-built. The custom-made inflation setup for this study is schematically presented in Fig. 2(a). Briefly, custom-made latex tubes (see Supplementary Methods for details) and tissue specimens with pre-imposed tears were mounted vertically onto coaxial needles and submerged within an acrylic tank filled with phosphate buffered saline (PBS, pH 7.4, Dot Scientific, Burton, MI) as shown in Fig. 2(b)–(d). The latex tubes were inflated via a computer-controlled syringe pump (accuracy: ±1%, New Era Pump Systems Inc., Farmingdale, NY) with infusion of PBS through plastic tubing. Pressure within the latex tubes was measured using a pressure transducer (max capacity: 345 kPa, accuracy: ±0.03%, Omega Engineering, Norwalk, CT), interfaced with a computer via a myDAQ device (accuracy: ±0.5% + 20 mV, National Instruments, Austin, TX). The transducer was aligned to the height of the latex tubes and tissue specimens to minimize the pressure differential due to fluid height. The needles holding the vaginal tissue specimens were fixed preventing axial extension, and they were arranged such that the top needle was connected to a load cell (accuracy: ±0.15%, LSB200 5 lb, Futek, Irvine, CA) mounted onto a linear motorized stage (XSlide XN10-0040-E04-71, Velmex Inc., Bloomfield, NY) while the bottom needle was fixed to a raised platform within the tank. High resolution images of the surface of the vaginal tissue specimens were taken using two CMOS cameras (Basler ace acA2440-75 um, Basler, Inc., Exton, PA) equipped with c-mount lenses (Xenoplan 2.8/50, Schneider Optics Inc., Hauppauge, NY). Non-contact strain measurements were performed with a 3D-DIC system (Vic-3D 8, Correlated Solutions, Columbia, SC).

2.3. Tear propagation inflation protocol

For mounting, each tissue specimen was pulled over two O-rings that were bonded with cyanoacrylate adhesive 2 mm away from the ends of two opposite 6-gauge stainless steel dispensing needles. The ends of the vaginal tissue specimen were secured to the needles with nylon thread and taped with Teflon tape (Fig. 2(c) and (d)). Following mounting, the axial length of the tissue specimen, *L*, was measured from the axial distance of its clamped ends via calipers (accuracy: ±0.1 mm, Mitutoyo Absolute Low Force Calipers Series 573, Japan). On average, the axial length of the tissue specimen was 14 ± 1 mm. The tissue specimen was then dyed with an aqueous methylene blue solution (1% w/v) and speckled with an aerosol fast dry gloss white paint to create a high contrast speckle pattern on its surface. The tissue specimen was continually hydrated with PBS throughout the mounting process.

Latex tubes ($n = 10$) were custom-made, lubricated with white lithium grease, mounted to the inflation setup, and subjected to a first inflation cycle, as described in the Supplementary Information. One of the two tissue-mounted needles was attached to the load cell on an actuator located outside the tank to easily lower the tissue-mounted needles into the tank and over the latex-mounted needles. The other tissue-mounted needle was then secured to a raised platform at the bottom of the tank (Fig. 2(a)). The tissue-mounted needles were vertically oriented with the introitus side at the bottom and the cervix side at the top so that the pre-imposed tear in the dorsal side of the vagina was centered within the field of view of the two CMOS cameras. The DIC system used for strain measurement was calibrated prior to testing via imaging of a plastic grid (10×14 mm^2 with 3 mm spacing) submerged within the tank. Images were imported into Vic-3D version 8 software (Correlated Solutions, Columbia, SC) and a 4th order variable ray origin model was implemented to correct for the changes in refractive indices due to imaging through media (PBS, acrylic, air). Images of the tissue surfaces were captured at a rate of 10 fps during testing.

An axial pre-load of 0.04 N was placed on the tissue specimens to remove any axial slack. The tissue specimen was then inflated by infusing PBS into the latex tube at a rate of 0.47 mL/min until it was completely torn. The volume of the PBS infused as well as the corresponding internal pressure and axial load were recorded. Once testing was complete, a subset of tissue specimens ($n = 3$) were removed from the tank, carefully dismounted from the needles, hydrated with PBS, wrapped in gauze, and frozen at 20 °C until ready for imaging.

2.4. SHG imaging

Second harmonic generation imaging was performed on two groups, each with three vaginas. Three vaginas from one group, the control group, were imaged but never subjected to inflation tests (Fig. 3(a)), while three vaginas from another group, the inflation-tested group, were imaged after inducing tear propagation via inflation tests as described above (Fig. 3(b)). Prior to imaging, all six tissue specimens were thawed in PBS at room temperature for 10 min, cut along the axial length of the vagina at the urethra (ventral side, Fig. 1), laid flat and bonded onto a Petri dish with cyanoacrylate adhesive, exposing the squamous epithelial layer. The dish was filled with PBS to maintain hydration throughout imaging. Tissue specimens were placed on a motorized stage of a Zeiss LSM 880 upright confocal microscope (Zeiss, Thornwood, NY). Backward-SHG imaging was performed with a Ti:Sapphire laser

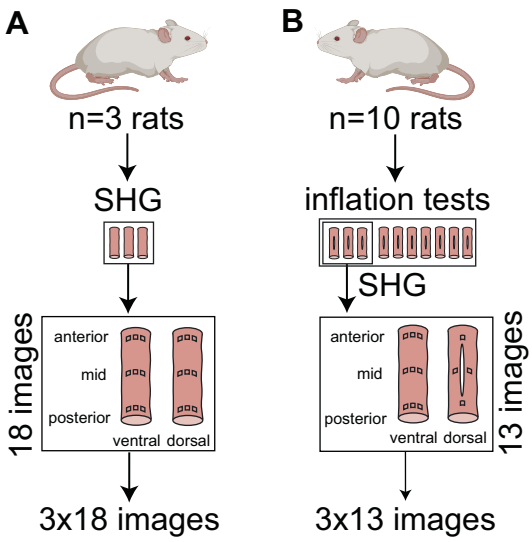

Fig. 3. Schematic of the two groups of rats used in this study. (a) Three vaginas from three rats were used only to collect SHG images. (b) Ten vaginas from ten rats were used for inflation testing. Three of the ten vaginas were also used to collect SHG images after inflation testing.

(Ultra 1, Coherent Inc., Santa Clara, CA). The laser produced linearly polarized, 140-fs duration pulses, spectrally centered at 780 nm at 80-MHz repetition rate. The beam deflected into the back port of the microscope and scanned across the tissue specimens by a galvanometric $x - y$ scanner. The beam then passed through a 690-nm short-pass dichroic mirror and focused onto the tissue specimens with a 40×, numerical aperture of 0.75, water-immersion microscope objective. The average excitation power illuminating the tissue specimen was kept to less than 30 mW, as measured by a power meter (1936-C, Newport Corp., Irvine, CA), to prevent any damage to the tissue specimens. The backscattered SHG signals from the tissue specimens traveled through the objective and were collected by a detector (BiG.2 module, Ziess, Thornwood, NY) after going through the 690-nm short-pass dichroic mirror, a secondary dichroic mirror, and finally a 390-nm bandpass filter (Semrock FF01-390/18-25, IDEX Health & Science, LLC, Rochester, NY). This process generated two-dimensional images (212.55×212.55 μm^2) from which the collagen fiber organization, including the fiber orientation, could be quantified.

Eighteen images ($m = 18$) were acquired for each vagina within the control (untested) group (Fig. 3(a)) and thirteen images ($m = 13$) were acquired for each specimen within the inflation-tested group, for a total of 93($= 18 \times 3 + 13 \times 3$) images (Fig. 3(b)). Six regions (anterior, middle, and posterior regions along the dorsal and ventral vaginal walls) were imaged in both the control (untested) group and inflation-tested group to investigate the potential region-dependent fiber response within the rat vagina as demonstrated within previous histomechanical studies on vaginal tissue [13,16,17]. For the control (untested) group, three images were obtained from the anterior (near the cervix), middle, and posterior (near the introitus) regions of both the dorsal (side near the rectum) and ventral (side near the urethra) vagina. For the inflation-tested group, three images were obtained for each of the anterior, middle, and posterior regions of the ventral vagina. The ventral side of the vagina was opposite to the dorsal side where a pre-imposed tear was created. For this reason, the regions in the ventral side were considered far from the tears. Finally, four images of the dorsal vagina, where tears occurred, were obtained: one image at each of the two tear tips located in the anterior and posterior regions of the vagina, and one image at each of the two sides of the tear in the middle region of the vagina (Fig. 3).

2.5. Data analysis

2.5.1. Tear propagation inflation test data

For each inflation test, the pressure and axial load contributions of the latex tube were estimated, as described in the Supplementary Information, and subtracted from the measured total pressure and axial load of the coaxial latex/tissue tube to compute the pressure and axial load of the vaginal tissue specimen.

Normalized tissue volume (NTV) was calculated as $\frac{V_o+V_{PBS}}{V_t}$, where V_o was the initial volume that was enclosed by the latex tube, computed using the inner radius, r, and axial length, l, of the latex tube (Supplementary Table 2), and the volume occupied by the sections of the 6-gauge needles that held the tissue specimen, V_{PBS} was the volume of PBS that was infused into the setup, and V_t was the initial volume that was enclosed by the tissue specimen computed from the inner radius, R, and axial length, L, of the vagina. During each inflation test of the tissue specimen, the only volume that changed was V_{PBS}.

Local normal Lagrangian strains in the hoop and axial directions were obtained from the dorsal side of the vagina where the tears were located. The average values of these local strains were calculated over several smaller regions of interest around the tear, resulting in a single average normal Lagrangian strain in the hoop direction and a single average normal Lagrangian strain in the axial direction within each region of interest for each recorded frame of testing. Five regions of interest within each tissue specimen were analyzed in total: a small circular region at each tip of the tear, a small circular region on either side of the mid-region of the tear, and a quadrilateral region enclosing (but not including) the tear.

Measurements of the tear geometry and propagation for each tissue specimen were performed within ImageJ (NIH, Bethesda, MD). Specifically, using the fit ellipse tool, measurements of the lengths of the major and minor axes, area, and circularity of the tears were calculated up to the point of initial tear propagation, $TP_{initial}$. The rates of increase for the major and minor axes were computed by dividing the increase in length over the increase in NTV. Moreover, the tear propagation toward the introitus, da_i, and the tear propagation toward the cervix, da_c, were measured as the axial distance between the tear tips at $TP_{initial}$ and new tear tips that were created with inflation. The rates of propagation were calculated up to the maximum pressure, $P_{\max}$, and beyond $P_{\max}$ by dividing the change in tear propagation toward the introitus and the cervix by the change in normalized pressure, $\frac{P}{P_{\max}}$.

2.5.2. SHG imaging

The orientation of collagen fibers within each of the collected 93 images were quantified by means of spatial Fourier analysis within a custom Matlab script [30–32]. Briefly, each image was subdivided into a 51×51 grid ($\sim 4 \times 4$ μm^2) with the size of the subdivisions determined by the collagen fiber size. A collagen fiber orientation value was computed for each grid, resulting in 2601 orientation values for each image. Using circular statistics, average orientations and circular variances were calculated for each anatomical region: dorsal anterior, middle, and posterior as well as ventral anterior, middle, and posterior regions for the control (untested) group and dorsal (near tear) anterior, middle, and posterior as well as ventral (away from tear) anterior, middle, and posterior regions for the inflation-tested group (Fig. 3).

2.6. Statistical analysis

All statistical data analysis was performed in a statistical software package (SPSS Statistics Subscription; IBM Corp., Armonk,

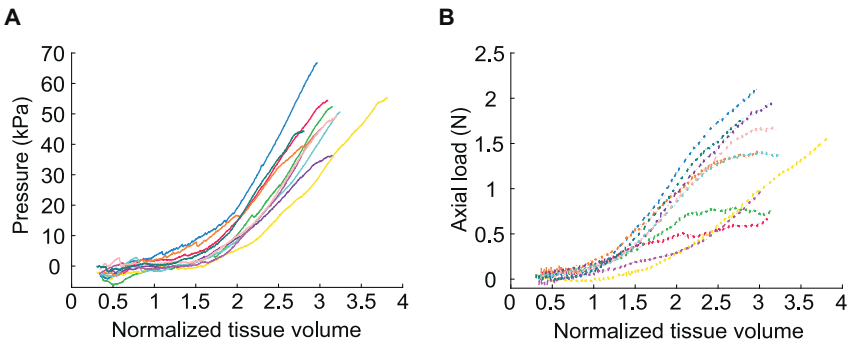

Fig. 4. (a) Pressure and (b) axial load versus normalized tissue volume (NTV) collected up to maximum pressure, $P_{max}-$ during inflation tests of rat vaginal tissue specimens ($n = 10$). Pressure and axial load versus NTV data from the same specimen are represented using the same color.

NY). The average hoop and axial strains were compared across five regions of interest at NTVs of 1, 1.5, 2, and 2.5 with a three-way repeated measures ANOVA. For this statistical analysis, there were 3 factors (NTV, direction, and region) with 4 levels for the NTV (1, 1.5, 2, and 2.5), 2 levels for the direction (hoop and axial directions) and 5 levels for the region (two regions at the two tips of the tear, two regions in the mid-region of the tear, and one quadrilateral region enclosing but not including the tear). The hoop and axial strains were further compared across five regions at $TP_{initial}$ and P_{max} via a three-way repeated measures ANOVA. For this analysis, there were 3 factors (time point during testing, direction, and region) with 2 levels for the time point during testing ($TP_{initial}$ and P_{max}), 2 levels for the direction (hoop and axial directions), and 5 levels for the region (two regions at the two tips of the tear, two regions in the mid-region of the tear, and one quadrilateral region enclosing the tear). No outliers were present for any factor and level combination of the two above factorial designs as determined by studentized residuals (residuals within ±3). Deviations from normality were present as determined by the Shapiro–Wilk's test of normality. A series of power transformations based on the Box-Cox transformation were used to attempt to correct the data. However, no optimal power transform ensured normality. The ANOVA procedures were carried out regardless with the original data as the ANOVA is fairly robust to deviations from normality. Any violations of sphericity were addressed by the Greenhouse–Geisser correction. Significant interactions were followed up by examining simple main effects via one-way repeated measures ANOVAs. Pairwise comparisons with a Bonferroni correction followed significant simple main effects where the Bonferroni correction was applied by multiplying the uncorrected p-value from the statistical test by the number of comparisons rather than dividing the α-level. The rate of length increase for the major and the minor axes of the preimposed tear per unit NTV as well as the magnitude and rate of tear propagation toward the cervix and introitus per unit NTV were compared using paired t-tests. The assumptions for the paired t-test (no outliers and normality of the differences) were satisfied. All data reported are mean ± standard deviation (std. dev.) unless otherwise stated and statistical significance was set to $p < 0.05$.

3. Results

3.1. Nonlinear and inhomogeneous finite strain response to inflation

Inflation of vaginal tissue specimens to complete failure progressed through three phases: initial pressurization and stretching, slow tear propagation up to P_{max}, and rapid tear propagation to complete failure. Vaginal tissue pressure and axial load data versus NTV data up to P_{max} are shown in Fig. 4(a) and (b). The pressure and axial load responses were both nonlinear, but the pressure responses were more consistent across tissue specimens relative to the axial load responses. The average maximum pressure was 50 ± 8 kPa and the corresponding average axial load at P_{max} was 1.4 ± 0.5 N (Table 1).

Table 1
Mean (±std. dev.) of measured quantities at the initial tear propagation, $TP_{initial}$, and maximum pressure, P_{max}, during inflation tests of rat vaginal tissue specimens ($n = 10$). Hoop and axial strains were computed from the region enclosing but not including the tear.

Measured quantity	$TP_{initial}$	P_{max}
Pressure (kPa)	40 ± 10	50 ± 8
Axial load (N)	1.2 ± 0.5	1.4 ± 0.5
Volume infused (mL)	0.7 ± 0.1	0.8 ± 0.1
Normalized tissue volume (NTV)	2.7 ± 0.3	3.1 ± 0.3
Hoop strain	0.7 ± 0.2	0.8 ± 0.3
Axial strain	0.08 ± 0.07	0.1 ± 0.1

Average hoop and axial strains at NTVs of 1, 1.5, 2, and 2.5 measured from five regions around the tear of tissue specimens are reported in Fig. 5(a) and (b). These NTVs were selected for comparison as all vaginas tested reached a NTV of 2.5, prior to $TP_{initial}$. $TP_{initial}$ presented, on average, at a NTV of 2.7 ± 0.3 (Table 1). Across all regions and levels of NTV, hoop strains were significantly larger than axial strains with a maximum p-value of 0.003 occurring between hoop and axial strains above the tear at a NTV of 1. As expected both hoop and axial strains increased for each region with increasing NTV (Fig. 5(a) and (b)). When hoop strains were compared between regions, no significant differences were observed at any level of NTV (Fig. 5(a)). Comparing axial strains between regions, a few significant differences were observed at each level of NTV as shown in Fig. 5(b). The increase in hoop strain from one NTV level to the next NTV level for each region was statistically significant (Fig. 6), with the exception of the hoop strain in the region right of the tear from 2 to 2.5 ($p = 0.056$) (Fig. 6(d)). No significant differences in axial strain were observed with increasing NTV for the regions above (closer to the cervix), below (closer to the introitus), or fully enclosing the tear (Fig. 6(a), (b) and (e)). In contrast, significant differences in axial strain were observed for the regions left and right of the tear where axial strains significantly increased with increasing NTV (Fig. 6(c) and (d)). Specifically, axial strains left of the tear at NTVs of 1.5, 2, and 2.5 were significantly larger than the axial strain at a NTV of 1 ($p = 0.014$, $p = 0.023$, and $p = 0.027$, respectively), while axial strains right of the tear significantly increased between every level of NTV.

Average hoop and axial strain data for the five aforementioned regions at $TP_{initial}$ and P_{max} are shown in Fig. 5(c) and (d). Hoop strains at regions above, below, and enclosing but not including the tear significantly increased from $TP_{initial}$ to P_{max} ($p = 0.003$, $p = 0.004$, and $p = 0.011$, respectively). The hoop strains

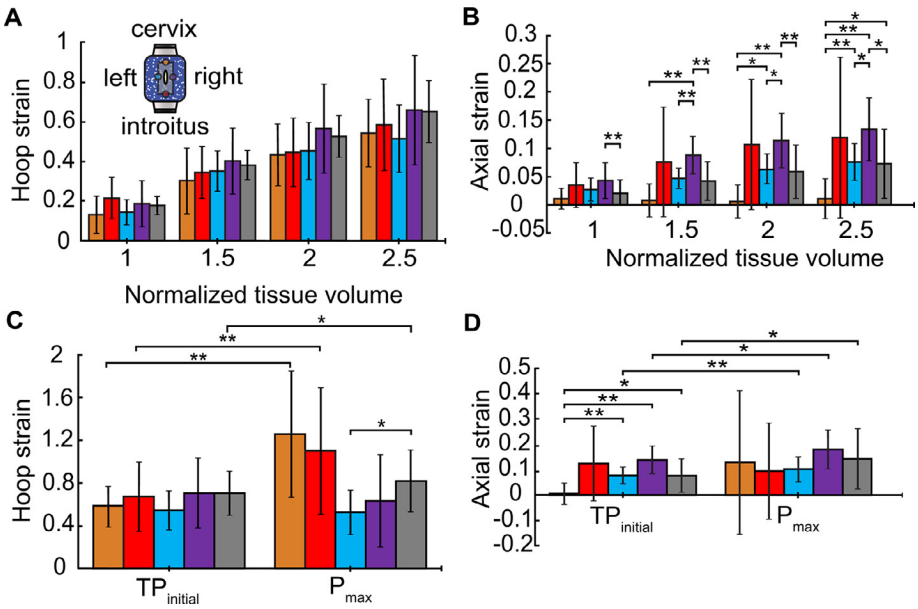

Fig. 5. Digital image correlation strain data from inflation tests compared by region and normalized tissue volume (NTV). Different colors denote different regions as shown in the insert: orange and red denote small circular regions at tips of the tear closer to the cervix and introitus, respectively, blue and purple denote small circular regions on left and right sides of the mid-region of the tear, respectively, and grey denotes a quadrilateral region enclosing (but not including) the tear. (a) Mean (±std. dev.) Lagrangian hoop strain and (b) mean (±std. dev.) Lagrangian axial strain measured at NTVs of 1, 1.5, 2, and 2.5 across five regions (as shown in the insert) around the tear of rat vaginal tissue specimens ($n = 10$). For clarity, only statistical differences across regions are reported. (c) Mean (±std. dev.) Lagrangian hoop strain and (d) mean (±std. dev.) Lagrangian axial strain at the initial tear propagation, $TP_{initial}$, and the maximum pressure, P_{max}, across the same five regions around the tear. Statistical differences across regions and between P_{max} and $TP_{initial}$ are reported. $^{*}p < 0.05$, $^{**}p < 0.01$. (For interpretation of the references to color in this figure legend, the reader is referred to the web version of this article.)

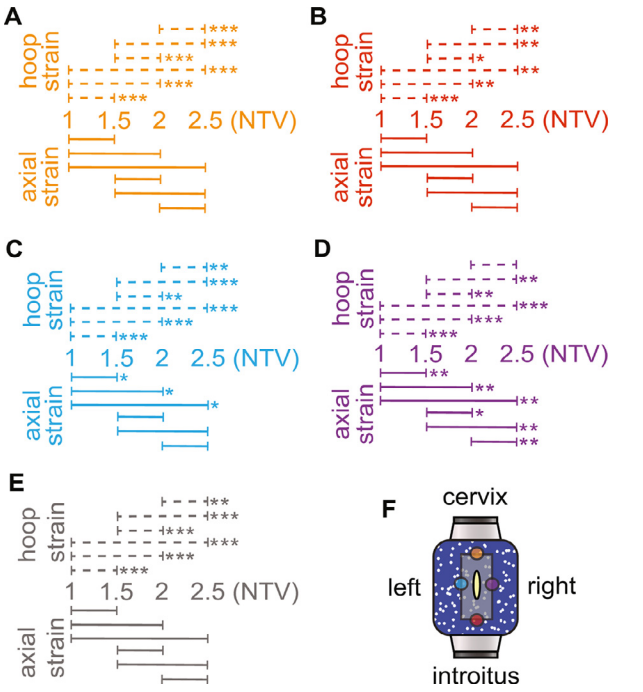

Fig. 6. Statistical comparison of hoop strains (dashed lines) and axial strains (continuous lines) between normalized tissue volumes (NTVs) of 1, 1.5, 2, and 2.5 for (a) and (b) small circular regions at tips of the tear closer to the cervix and introitus, respectively, (c) and (d) small circular regions on left and right sides of the mid-region of the tear, respectively, and (e) quadrilateral regions enclosing (but not including) the tear. (f) Regions around the tear, where (hoop and axial) strains were compared between NTVs, are displayed in orange, red, blue, purple, and grey. $^{*}p < 0.05$, $^{**}p < 0.01$, $^{***}p < 0.001$. (For interpretation of the references to color in this figure legend, the reader is referred to the web version of this article.)

left and right of the tear decreased from $TP_{initial}$ to P_{max}, but this was not a significant decrease ($p = 0.418$ and $p = 0.151$, respectively). Comparing the hoop strains by region for $TP_{initial}$, no significant differences were observed, but for P_{max}, a significant difference between the region right of the tear and the region enclosing the tear was observed ($p = 0.046$). Axial strains for the regions above, left of, right of, and enclosing the tear all increased from $TP_{initial}$ to P_{max} with significant differences arising for the regions left of, right of, and enclosing the tear ($p = 0.009$, $p = 0.027$, and $p = 0.023$, respectively). At $TP_{initial}$, the axial strains for the regions left of, right of, and enclosing the tear were significantly larger than the axial strains above the tear ($p = 0.002$, $p = 0.003$, and $p = 0.018$, respectively), while no significant differences in axial strain were observed between regions at P_{max}. Across all regions for both $TP_{initial}$ and P_{max}, the hoop strains were significantly larger than the axial strains with a maximum p-value of 0.012 between hoop and axial strains right of the tear at P_{max}.

3.2. Tear geometry and propagation response to inflation

The changes in shape of axially oriented, pre-imposed tears with increases in NTV during inflation are displayed in Fig. 7. These data were collected up to the point of $TP_{initial}$. The initial shape of the tears generally resembled narrow ellipses with the major and minor axes oriented along the axial and hoop directions, respectively. The average initial length of the major axis was 3.1 ± 0.2 mm, the average initial length of the minor axis was 0.6 ± 0.3 mm, and the average initial area was 1.4 ± 0.7 mm^2. As can be observed in Fig. 7(a) and (b), the length of the minor axis increased at a faster rate than the length of the major axis resulting in a decreased eccentricity of the tears. This can also be noted in Fig. 7(c) and (d) where the tear area and circularity ($= 4\pi$ area/perimeter^2) of the tears increased with increasing NTV. On average, the rate of length increase for the major and minor

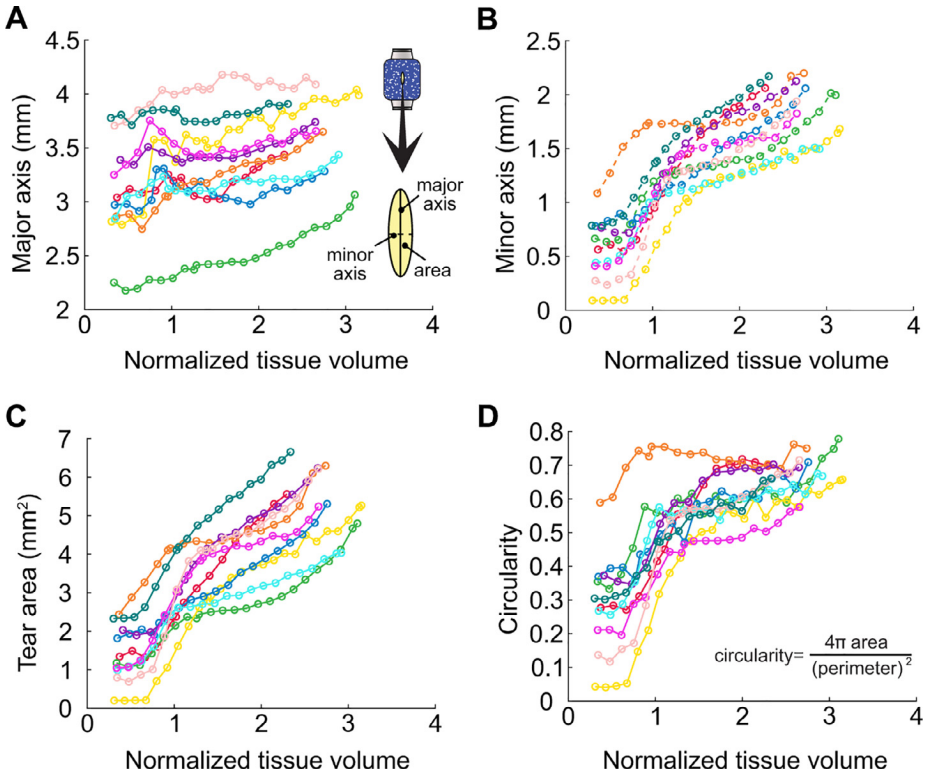

Fig. 7. Evolution of the pre-imposed, elliptical tear geometry during inflation tests of rat vaginal tissue specimens ($n = 10$) before tear propagation is observed. (a) Major axis, (b) minor axis, (c) area, and (d) circularity of the pre-imposed, elliptical tears versus normalized tissue volume (NTV). Data from the same specimen are represented using the same color.

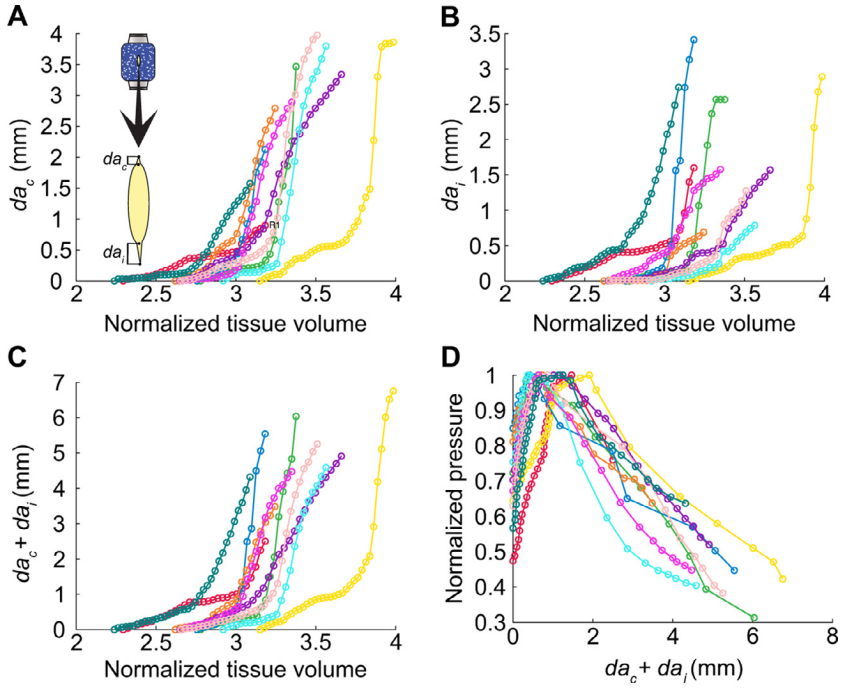

Fig. 8. Evolution of tear propagation during inflation tests of rat vaginal tissue specimens ($n = 10$). (a) Tear propagation toward the cervix (da_c), (b) tear propagation toward the introitus (da_i), and (c) total tear propagation ($da_c + da_i$) versus normalized tissue volume (NTV). (d) Pressure normalized by the maximum pressure achieved, P_{max}, versus total tear propagation ($da_c + da_i$). Data from the same specimen are represented using the same color.

axes were 0.2 ± 0.1 mm and 0.6 ± 0.1 mm per unit NTV, respectively. The difference between these rates was statistically significant ($p < 0.0005$). In effect, the tips of the tears became round as the circularity, on average, changed from 0.3 ± 0.1 to 0.70 ± 0.06. At $TP_{initial}$, the average length of the major axis was 3.6 ± 0.3 mm, the average length of the minor axis was 2.0 ± 0.2 mm, and the average area of the tear was 5.6 ± 0.8 mm^2.

Once a tear in the vagina was observed to propagate, the increase in length of the tear was measured up to and beyond P_{max}. Propagation consistently occurred along the axial direction at both the upper (toward the cervix) and lower (toward the introitus) tips

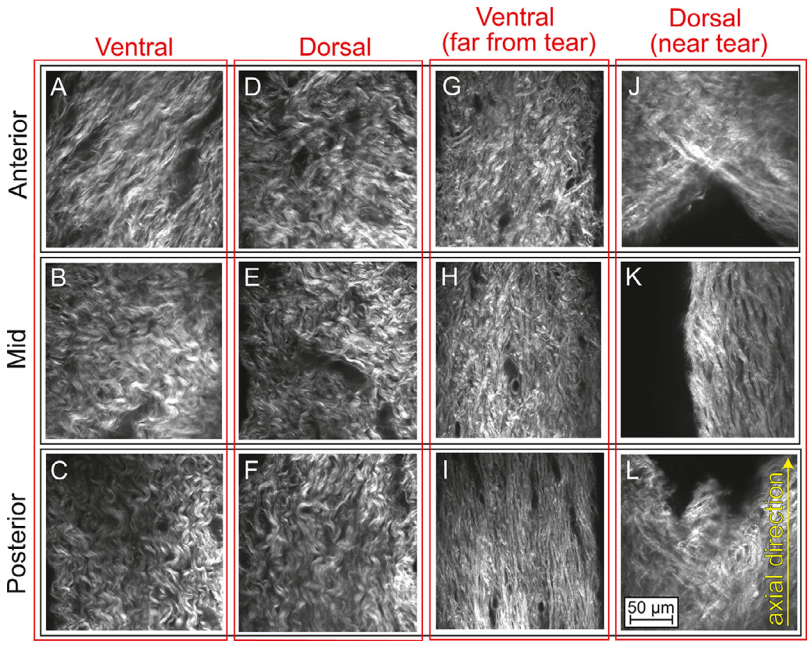

Fig. 9. Representative SHG images of the collagen fibers within six different regions from (a)–(f) the control (untested) rat vaginal tissue specimens and (g)–(l) the inflation-tested rat vaginal tissue specimens. Data were collected as shown in Fig. 3(a) and (b), respectively.

of the pre-imposed tears. Initially, the tear propagation was found to proceed slowly with increasing NTV (Fig. 8(a)–(c)). A more rapid propagation of the tear was observed after achieving P_{max}, at an average NTV of 3.1 ± 0.3 (Table 1). Fig. 8(a) displays the propagation of tears toward the cervix (da_c), Fig. 8(b) displays the propagation of tears toward the introitus (da_i), and Fig. 8(c) displays the total propagation of the tears ($da_c + da_i$) versus NTV. On average, da_i at P_{max} was 0.6 ± 0.4 mm while da_c at P_{max} was 0.4 ± 0.2 mm. This difference was not statistically significant ($p = 0.130$). In addition, pressure data for each vaginal tissue specimen, normalized by P_{max}, versus the total propagation of the tear is presented in Fig. 8(d). On average, tear propagation was observed to begin at $70 \pm 10\%$ of P_{max}, indicating localized damage prior to large tear propagation. At P_{max}, the tears propagated on average 1.0 ± 0.5 mm in the axial direction (Fig. 8(d)). The rate of tear propagation up to P_{max} was on average 3 ± 1 mm per unit normalized pressure while the rate of tear propagation beyond P_{max} was on average 9 ± 5 mm per unit normalized pressure. This difference in rates was statistically significant ($p < 0.005$).

3.3. Collagen fiber morphology before and after tear propagation inflation tests

The collagen fiber organization of rat vaginal tissue was examined at several different anatomical locations within the tissue specimens from the control (untested) group ($n = 3$) (Fig. 9(a)–(f)) and within tissue specimens from the inflation-tested group ($n = 3$) (Fig. 9(g)–(l)). Collagen fibers within control (untested) specimens were observed to be undulated and disorganized. Following inflation testing, collagen fibers were markedly straightened and aligned toward the axial direction within the ventral posterior region (Fig. 9(i)). The collagen fibers in the mid and anterior ventral regions maintained some undulation and disorganization, but there was a noticeable general reorientation of collagen fibers in the axial direction (Fig. 9(g) and (h)). Collagen fibers in the dorsal region (Fig. 9(j)–(l)) reoriented tangentially to the surface of the axially oriented tear. In the anterior and posterior regions, where the tips of the tears were located, collagen fibers formed a crossing pattern (Fig. 9(j)–(l), and in the mid region they aligned parallel to the tear (Fig. 9(k)).

Average orientations and circular variances of collagen fibers from control (untested) and inflation-tested tissue specimens are reported in Fig. 10(a)–(f) and (g)–(l), respectively, where 90° represents the axial direction. For untested specimens, data from the anterior and mid regions of the ventral and dorsal walls of the vagina showed collagen fiber alignment predominately between 45° and +45° (Fig. 10(a), (b) and (d), (e)). Specifically, the dorsal walls appeared to have two main preferred fiber directions within this range (Fig. 10(d) and (e)) whereas the ventral wall had a single preferred direction (Fig. 10(a) and (b)). The posterior regions of the ventral and dorsal walls showed collagen fibers aligned about single preferred directions of approximately 117° and 70°, respectively (Fig. 10(c) and (f)).

Noticeable differences in the fiber orientation of inflation-tested tissue specimens relative to control (untested) tissue specimens were observed within every region (Fig. 10). For the inflation-tested specimens, within the anterior ventral region (far from the tear), the collagen fibers were primarily aligned along two preferred orientations around ±60° (Fig. 10(g)). In the mid and posterior regions, the collagen fibers exhibited axially preferred orientations of 80° and 96°, respectively (Fig. 10(h) and (i)). In the anterior and posterior dorsal (near the tear) regions, the collagen fibers had average orientations of 3° and 30°, respectively (Fig. 10(j)–(l)). The fibers in these regions were generally oriented in the hoop direction, perpendicular to the direction of tear propagation. In the mid dorsal (near the tear) region, the average orientation of collagen fibers was 100° and the fibers were generally oriented in the axial direction (Fig. 10(k)).

4. Discussion

While a few investigators have studied the tear propagation of soft collagenous tissues [22–29], this is the first experimental study to characterize the tear propagation in vaginal tissue under a biaxial state of stress. Unlike our previous planar biaxial tests [19], these new tests were conducted so as to preserve the in vivo

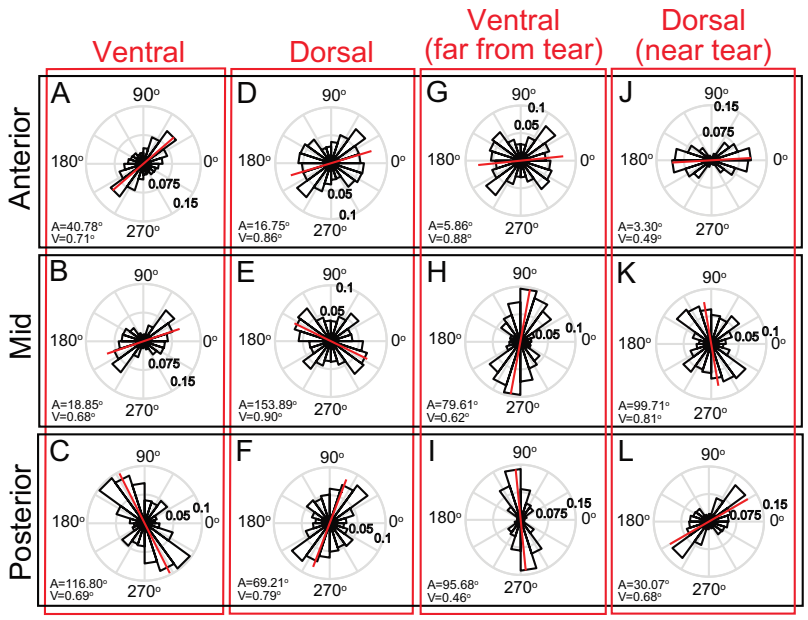

Fig. 10. Polar histograms of collagen fiber orientations in degrees for the (a)–(f) control (untested) and (g)–(l) inflation-tested rat vaginal tissue specimens in different anatomical regions, with 90° representing the axial direction of the vagina. In each region, radial values represent the frequencies of orientation occurrences (i.e., 0.05 = 5%, 0.075 = 7.5%, 0.1 = 10%, 0.15 = 15% of the total fibers). The average orientation is represented by a solid red line at the center of each polar histogram. Red labels and frame boxes are used for the ventral and dorsal regions and black labels and boxes for the anterior, mid, and posterior regions. Data were collected from 54(= 18 × 3) images from $n = 3$ rats for the control tissue specimens and from 39(= 13 × 3) images from $n = 3$ rats for the inflation-tested tissue specimens as shown in Fig. 3(a) and (b), respectively. (A = average orientation and V = circular variance). (For interpretation of the references to color in this figure legend, the reader is referred to the web version of this article.)

tubular geometry of the vagina. Toward this end, we custom-made an inflation setup to pressurize axially fixed rat vaginas with pre-imposed, axially oriented tears of ~ 3 mm in length via latex tubes. The maximum pressure sustained by the rat vagina before large tear propagation was approximately 50 kPa, less than half the pressure required to generate tearing [21]. Throughout inflation testing, the strain field was measured using the DIC technique, and the hoop strains were always found to be significantly larger than the axial strains. The tears, which had an initial elliptical shape, became more circular under pressure, had no significant difference in propagation toward the introitus versus the cervix at maximum pressure and propagated rapidly once the maximum pressure was achieved.

In addition to inflation testing, we performed SHG microscopy to reveal, for the first time, the collagen fiber organization in the rat vagina and the alterations that were induced by inflation. The collagen fiber orientation varied by anatomical regions, with the collagen fibers reorienting and becoming straight due to inflation. The collagen fibers created an inherent protective mechanism slowing the progression of tearing in the vaginal tissue. Consistent with other tear propagation studies [19,25,26,28,33], vaginal tears blunted prior to the onset of propagation.

The pressure data recorded during inflation testing were remarkably consistent across vaginal tissue specimens whereas the axial load data were found to exhibit some variability (Fig. 4(a) and (b)). This variability may be the result of some inevitable mismatch between the axial length of the latex tubes and the tissue specimens, as well as some friction at the latex/tissue interface. White lithium grease was employed to minimize contact friction, but the proximity to a perfect slip condition is unknown. Variability in the axial load data could also be due to the difference between the axial length of the tissue specimens relative to the in vivo axial length of the vagina. As previously demonstrated for arteries [34,35] and, more recently, for the murine vagina [20], inflation at a fixed axial length greater than the in vivo axial length resulted in an increase in axial tension, while inflation at a fixed axial length smaller than the in vivo axial length led to a decrease in axial tension. The in vivo axial length of the tissue specimens was not recorded in this study and its influence on the *ex vivo* mechanical response of the vagina should be further investigated.

The DIC method is a powerful optical technique that has enabled us to capture the highly inhomogenous strain field in the vagina. Taking full advantage of this technique, comparisons of strain fields across several regions around the pre-imposed tears were made (Fig. 5). Similar to our previous study [21], hoop strains were always significantly larger than axial strains throughout inflation testing, as would be expected for the specimen, which was fixed in axial length. Furthermore, hoop strains were not significantly different by region but significantly increased with inflation, suggesting that the radial expansion of the vaginal tissue was region independent (Fig. 5(a)). On the contrary, the axial strains varied across regions and did not always increase significantly with inflation (Fig. 5(b)). At the maximum pressure, a significant increase in hoop and axial strains were observed when compared to the strains at the initial tear propagation (Fig. 5(c) and (d)), as one might have expected. However, the hoop strains significantly increased above and below the tear (Fig. 5(c)) while the axial strains significantly increased left and right of the tear (Fig. 5(d)). This distribution of strain around the axially oriented tear as the tear propagated was consistent with the alignment of collagen fibers around the tear after inflation testing (Fig. 9(j)–(l)).

Measurements of minor and major axes, area, and circularity of the tear during inflation detailed the increase in size of the tear as the vagina was pressurized but also the progressive rounding of the initially elliptically shaped tear (Fig. 7). These findings are, however, only for tears that form in the mid dorsal region of the vagina. Comparable tear propagation up to maximum pressure was observed in the posterior and anterior regions of the vagina,

suggesting that the blunting mechanisms were similar in these regions (Fig. 8(a) and (b)). Thus, we speculate that vaginal tears that occur closer to the introitus and cervix may propagate similarly. Tear propagation prior to the maximum pressure was small and occurred at a slower rate relative to tear propagation beyond the maximum pressure for tears with major axis oriented along the axial direction (Fig. 8(d)). It is possible that these propagation rates increase for tears with major axis oriented along the hoop direction since such tears deform significantly more [19]. However, propagation of such tears could be also redirected from the hoop direction to the axial direction as the axially oriented fibers in the vagina may act as barriers. This redirection would again take more energy and could decrease the rate of propagation of such tears significantly.

Considering the strain results along with the SHG imaging and analysis (Fig. 9), the strain inhomogeneity can partly be attributed to the local variations in collagen fiber microstructure, where the initially disorganized and wavy collagen fibers primarily reoriented toward the axial direction to provide axial stiffness and hoop compliance. The reorientation of fibers toward the axial direction under a state of biaxial stress, despite significantly larger hoop strains, may signal a preferential alignment linked to the physiology of the vagina. A primary function of the vagina is to expand, and the alignment of fibers in the axial direction would serve to allow such radial expansion. Moreover, the dispersion of collagen fibers about the hoop direction toward the cervix, in the anterior region, may be necessary for maintaining connection to the cervix. One must be mindful of the conclusions that could be drawn here as imaging was not performed during testing but after testing and, while regional dependent changes in the collagen microstructure were observed before and after inflation, specific correlations between the fiber organization and local strains are unknown. Moreover, the rate at which collagen fibers were recruited, straightened, and reoriented was not captured, and it could be region dependent and further explain the inhomogenous strain field of the vaginal tissue. Finally, limitations of the commercial system used for SHG, as detailed later, require that the interpretation of fiber orientations and distributions be considered in a more qualitative rather than quantitative manner (e.g., the difference in average orientations of 70° and 110° between two distributions is not necessarily meaningful but rather should be interpreted as distributions with average orientations in the general axial, 90°, direction). Because tears in the vagina always formed in the axial direction in our previous study [21], we decided to pre-impose tears in such direction to analyze their behavior under inflation. However, the tear behavior in the radial direction should also be investigated since we often observed layer de-lamination with tears that initiate in the intima layer [21]. Ring vaginal tissue specimens could be tested using our custom-built testing apparatus in order to analyze the through-thickness tear behavior in the radial-circumferential plane, as done by Haslach et al. [29] for bovine aortas. By integrating the results of different tests, one would be able to better classify the type of fracture mode (mode I, mode II, and/or mode III) of the vaginal tissue.

Although our ex vivo inflation tests characterize the mechanical response of vaginal tissue better than uniaxial and planar biaxial tests, they do not account for the in vivo physiological loading conditions of the vagina. For example, in our study the vaginal tissue was isolated from the surrounding muscle and connective tissues that are likely to play important roles in the propagation of vaginal tears. Our tests were performed on passivated vaginal specimens, without considering the contractions that are caused by the muscularis layer of the vagina [36]. This layer is composed of smooth muscle cells that induce contractions of the vagina in both the axial and hoop directions as shown in our recent study [18]. Such contractions could significantly influence the tear propagation mechanisms of the vagina in vivo. Finally, the vaginal specimens were subjected to multiple freeze-thaw cycles and this practice may have altered the tear propagation mechanism. However, we speculate that the changes induced by the freeze-thaw cycles were minimal based on published studies on the effect of freezing on the mechanical properties of the ewe vagina and, more recently, on rat tail tendon fascicles [37,38].

SHG microscopy represents the gold standard method for imaging collagen fibers within vaginal tissue. Our results have shown, for the first time, the collagen fiber architecture of the rat vagina within the ventral and dorsal regions, anterior, mid, and posterior regions, as well as regions far from and near to the tear. However, all the images were always collected at one in-depth through-thickness location. Because the vagina is composed of four layers and our study suggested that de-lamination may be one of the mechanisms of tear propagation, SHG images should be collected across several in-depth through-thickness locations in the various layers. We attempted this but it resulted to be quite challenging and time consuming leading to swelling of the vaginal tissue during imaging. The swelling altered the focal plane of the light beam within the tissue during image acquisition and prevented the use of through-thickness, three-dimensional fiber analysis. Moreover, we used a commercial system for our SHG microscopy, which generated linear polarization and only allowed for backward SHG signal acquisition. The use of linear polarization, rather than the preferred circular polarization, may have skewed our results. Similarly, the collagen fibers may have appeared punctate in images derived from back-scattered SHG signal, in contrast to their forward-scattered counterpart [39]. More research is required to understand the differences between the forward and backward SHG images of collagen fibers, especially given the potential clinical impact of backward SHG imaging for vaginal tear detection.

Rats have long served as the primary animal models for studies on the mechanical properties of the vagina due to their close histological similarity to humans. The layered structure of the vagina is, for example, common to rats and humans. Still we do not know whether the collagen fiber organization in the different layers and anatomical regions of the vaginal wall is comparable across the two species. We have shown in this study that such organization governs the mechanical and tearing behavior of the rat vaginal tissue. For this reason, the relevance and applicability of our mechanical and micro-structural results to humans will be better investigated once new data on human vaginal tissue are collected. Nonetheless, this study filled out major gaps in our knowledge about the microstructure and mechanics of the vagina and provided new ideas on the experimental methods that can be used to enhance the relevance of animal models to women's reproductive health.

Bipedalism and encephalization have made parturition in humans much more complicated than parturition in any other living species: bigger babies with larger brains need to move through vaginas in narrower pelves [40]. Thus, there are no other species that experience maternal trauma and tearing like women do. Although the vaginal tissue changes significantly with pregnancy and parturition to accommodate the passage of a full-term baby, the vaginal tissue remodeling in humans has yet to be characterized. In rats, the vaginal tissue becomes more complaint [41,42] and the elastic fibers become wavier [42] during pregnancy and parturition, so tears in pregnant vaginal tissue may propagate following a different mechanism that the one presented here for virgin rats. For this reason, future experiments using the experimental methods presented in this manuscript should investigate the tear propagation mechanism at various gestation time points in the rat to reveal the effect of pregnancy and parturition on tear propagation. This is especially important since tears in the human vagina pri-

marily present during vaginal delivery, though they also happen during sexual activity [43].

The long-term goal of this research is to develop quantitative and objective methods for predicting and evaluating vaginal tears. Accurate prediction of tear formation could not only reduce maternal trauma but also decrease unnecessary caesarean deliveries. Indeed, the current risk-factors (primiparity, forceps or vacuum delivery, birth weight greater than 4 kg, episiotomy, shoulder dystocia) are alone insufficient to predict maternal trauma and lead to the recommendation of caesarean deliveries, with increased risk of maternal death [44]. Early evaluation of large vaginal tears could serve to suggest immediate follow-up care and prevent future pelvic floor dysfunctions. Large vaginal tears during childbirth are clinical markers for trauma to the major supportive muscle of the pelvic floor, the levator ani [8]. Trauma to this important muscle is very common during vaginal delivery. However, it is often occult and very difficult to diagnose immediately after childbirth, leading to female pelvic organ prolapse in later life.

5. Conclusions

This experimental work provided the first characterization of the tear propagation properties of the vaginal tissue under a biaxial state of stress using the rat as animal model. An inflation setup that enabled the inflation of entire vaginas with pre-existing tears was custom-built and used in conjunction with the DIC method to capture the strain field around the tears. The pressure and axial load versus NTV responses of vaginal tissue was nonlinear, and the vaginal tissue exhibited heterogeneity in the strain field around a tear. Tears propagated along the axial direction of the vagina, slowly prior to the maximum pressure and more rapidly once the maximum pressure was achieved. SHG imaging revealed the wavy and disorganized morphology of the collagen fibers within the control (untested) tissue. Following inflation testing, collagen fibers were straightened, more uniformly aligned, and reoriented near to and far from the tears. Overall, the distribution of strain and orientation of collagen fibers around the tears indicated toughening of the vagina. These findings provide a more refined understanding of the mechanisms of vaginal tearing and have the potential to improve prevention and treatment strategies for maternal birth trauma.

Declaration of Competing Interest

The authors declare that they have no known competing financial interests or personal relationships that could have appeared to influence the work reported in this paper.

CRediT authorship contribution statement

Jeffrey A. McGuire: Conceptualization, Investigation, Methodology, Data curation, Formal analysis, Validation, Visualization, Writing - original draft, Writing - review & editing, Software, Supervision. **Jose L. Monclova:** Investigation, Methodology, Validation, Visualization. **Adriana C. Salazar Coariti:** Formal analysis, Resources, Software. **Caleb A. Stine:** Methodology, Resources, Software. **Kimani C. Toussaint Jr.:** Methodology, Formal analysis, Software, Writing - review & editing, Supervision. **Jennifer M. Munson:** Methodology, Resources, Supervision. **David A. Dillard:** Conceptualization, Methodology, Writing - review & editing, Funding acquisition. **Raffaella De Vita:** Conceptualization, Investigation, Methodology, Data curation, Formal analysis, Visualization, Writing - original draft, Writing - review & editing, Resources, Funding acquisition, Project administration, Supervision.

Acknowledgments

This work was supported by the National Science Foundation grant number 1929731 and the Institute for Critical Technology and Sciences at Virginia Tech. The authors would like to thank Dr. Sarah Clinton, Dr. Matthew Glover, Mr. Keaton Unroe, and Ms. Theresa Wallace for providing the rats for this study. They also would like to thank Drs. Anne Staples and Jonathan Boreyko for insightful discussions regarding the fluid mechanics within the experimental setup.

Supplementary material

Supplementary material associated with this article can be found, in the online version, at doi:10.1016/j.actbio.2021.03.065.

References

[1] E. Samuelsson, L. Ladfors, B.G. Lindblom, H. Hagberg, A prospective observational study on tears during vaginal delivery: occurrences and risk factors, Acta Obstet. Gynecol. Scand. 81 (1) (2002) 44–49.
[2] L.M. Hopkins, A.B. Caughey, D.V. Glidden, R.K. Laros, Racial/ethnic differences in perineal, vaginal and cervical lacerations, Am. J. Obstet. Gynecol. 193 (2) (2005) 455–459.
[3] A. Metcalfe, S. Tohill, A. Williams, V. Haldon, L. Brown, L. Henry, A pragmatic tool for the measurement of perineal tears, Br. J. Midwifery 10 (7) (2002) 412–417.
[4] A.K. Örnö, K. Maršál, A. Herbst, Ultrasonographic anatomy of perineal structures during pregnancy and immediately following obstetric injury, Ultrasound Obstet. Gynecol. 32 (4) (2008) 527–534.
[5] M. Fitzpatrick, C. O'Herlihy, Short-term and long-term effects of obstetric anal sphincter injury and their management, Curr. Opin. Obstet. Gynecol. 17 (6) (2005) 605–610.
[6] W. H. Organization, et al., The ICD-10 Classification of Mental and Behavioural Disorders: Diagnostic Criteria for Research, 2, World Health Organization, 1993.
[7] H.P. Dietz, A.V. Gillespie, P. Phadke, Avulsion of the pubovisceral muscle associated with large vaginal tear after normal vaginal delivery at term, Aust. N. Z. J. Obstet. Gynaecol. 47 (4) (2007) 341–344.
[8] K.L. Shek, K. Green, J. Hall, R. Guzman-Rojas, H.P. Dietz, Perineal and vaginal tears are clinical markers for occult levator ani trauma: a retrospective observational study, Ultrasound Obstet. Gynecol. 47 (2) (2016) 224–227.
[9] L.A. Smith, N. Price, V. Simonite, E.E. Burns, Incidence of and risk factors for perineal trauma: a prospective observational study, BMC Pregnancy Childbirth 13 (1) (2013) 1–9.
[10] H.P. Dietz, A.V.M. Franco, K.L. Shek, A. Kirby, Avulsion injury and levator hiatal ballooning: two independent risk factors for prolapse? An observational study, Acta Obstet. Gynecol. Scand. 91 (2) (2012) 211–214.
[11] K.T. Barnhart, A. Izquierdo, E.S. Pretorius, D.M. Shera, M. Shabbout, A. Shaunik, Baseline dimensions of the human vagina, Hum. Reprod. 21 (6) (2006) 1618–1622.
[12] L.C. Skoczylas, Z. Jallah, Y. Sugino, S.E. Stein, A. Feola, N. Yoshimura, P.A. Moalli, Regional differences in rat vaginal smooth muscle contractility and morphology, Reprod. Sci. 20 (4) (2013) 382–390.
[13] R. Rynkevic, P. Martins, L. Hympanova, H. Almeida, A. Fernandes, J. Deprest, Biomechanical and morphological properties of the multiparous ovine vagina and effect of subsequent pregnancy, J. Biomech. 57 (2017) 94–102.
[14] G.L. Clark, A.P. Pokutta-Paskaleva, D.J. Lawrence, S.H. Lindsey, L. Desrosiers, L.R. Knoepp, C.L. Bayer, R.L. Gleason Jr., K.S. Miller, Smooth muscle regional contribution to vaginal wall function, Interface Focus 9 (4) (2019) 20190025.
[15] R.V. Krstic, Human Microscopic Anatomy: An Atlas for Students of Medicine and Biology, Springer Science & Business Media, 2013.
[16] D. Ulrich, S.L. Edwards, V. Letouzey, K. Su, J.F. White, A. Rosamilia, C.E. Gargett, J.A. Werkmeister, Regional variation in tissue composition and biomechanical properties of postmenopausal ovine and human vagina, PLoS One 9 (8) (2014) e104972.
[17] D. Ulrich, S.L. Edwards, K. Su, J.F. White, J.A.M. Ramshaw, G. Jenkin, J. Deprest, A. Rosamilia, J.A. Werkmeister, C.E. Gargett, Influence of reproductive status on tissue composition and biomechanical properties of ovine vagina, PLoS One 9 (4) (2014) e93172.
[18] A. Huntington, E. Rizzuto, S. Abramowitch, Z.D. Prete, R. De Vita, Anisotropy of the passive and active rat vagina under biaxial loading, Ann. Biomed. Eng. 47 (2019) 272–281.
[19] J. McGuire, S.D. Abramowitch, S. Maiti, R. De Vita, Swine vagina under planar biaxial loads: an investigation of large deformations and tears, J. Biomech. Eng. 141 (4) (2019) 041003–041009.
[20] K.M. Robison, C.K. Conway, L. Desrosiers, L.R. Knoepp, K.S. Miller, Biaxial mechanical assessment of the murine vaginal wall using extension–inflation testing, J. Biomech. Eng. 139 (10) (2017) 104504.
[21] J.A. McGuire, C.L. Crandall, S.D. Abramowitch, R. De Vita, Inflation and rupture of vaginal tissue, Interface Focus 9 (4) (2019) 20190029.

[22] G. Fessel, J. Wernli, Y. Li, C. Gerber, J.G. Snedeker, Exogenous collagen cross-linking recovers tendon functional integrity in an experimental model of partial tear, J. Orthop. Res. 30 (6) (2012) 973–981.
[23] G.A.V. Forell, P.S. Hyoung, A.E. Bowden, Failure modes and fracture toughness in partially torn ligaments and tendons, J. Mech. Behav. Biomed. Mater. 35 (2014) 77–84.
[24] S.E. Szczesny, J.L. Caplan, P. Pedersen, D.M. Elliott, Quantification of interfibrillar shear stress in aligned soft collagenous tissues via notch tension testing, Sci. Rep. 5 (2015) 14649.
[25] W. Yang, V.R. Sherman, B. Gludovatz, E. Schaible, P. Stewart, R.O. Ritchie, M.A. Meyers, On the tear resistance of skin, Nat. Commun. 6 (2015) 6649.
[26] A.E. Ehret, K. Bircher, A. Stracuzzi, V. Marina, M. Zündel, E. Mazza, Inverse poroelasticity as a fundamental mechanism in biomechanics and mechanobiology, Nat. Commun. 8 (1) (2017) 1002.
[27] J.M. Peloquin, M.H. Santare, D.M. Elliott, Short cracks in knee meniscus tissue cause strain concentrations, but do not reduce ultimate stress, in single-cycle uniaxial tension, R. Soc. Open Sci. 5 (11) (2018) 181166.
[28] K. Bircher, M. Zündel, M. Pensalfini, A.E. Ehret, E. Mazza, Tear resistance of soft collagenous tissues, Nat. Commun. 10 (1) (2019) 792.
[29] H.W. Haslach Jr., A. Siddiqui, A. Weerasooriya, R. Nguyen, J. Roshgadol, N. Monforte, E. McMahon, Fracture mechanics of shear crack propagation and dissection in the healthy bovine descending aortic media, Acta Biomater. 68 (2018) 53–66.
[30] T.Y. Lau, H.K. Sangha, E.K. Chien, B.L. McFarlin, A.J.W. Johnson, K.C. Toussaint Jr., Application of fourier transform-second-harmonic generation imaging to the rat cervix, J. Microsc. 251 (1) (2013) 77–83.
[31] R.A.R. Rao, M.R. Mehta, S. Leithem, K.C. Toussaint Jr., Quantitative analysis of forward and backward second-harmonic images of collagen fibers using fourier transform second-harmonic-generation microscopy, Opt. Lett. 34 (24) (2009) 3779–3781.
[32] R.A.R. Rao, M.R. Mehta, K.C. Toussaint Jr., Fourier transform-second-harmonic generation imaging of biological tissues, Opt. Express 17 (17) (2009) 14534–14542.
[33] D. Taylor, N. O'Mara, E. Ryan, M. Takaza, C. Simms, The fracture toughness of soft tissues, J. Mech. Behav. Biomed. Mater. 6 (2012) 139–147.
[34] P. van Loon, W. Klip, E.L. Bradley, Length–force and volume–pressure relationships of arteries, Biorheology 14 (4) (1977) 181–201.
[35] W.W. von Maltzahn, R.G. Warriyar, W.F. Keitzer, Experimental measurements of elastic properties of media and adventitia of bovine carotid arteries, J. Biomech. 17 (11) (1984) 839–847.
[36] A. Huntington, K. Donaldson, R. De Vita, Contractile properties of vaginal tissue, J. Biomech. Eng. 142 (2020) 080801.
[37] C. Rubod, M. Boukerrou, M. Brieu, P. Dubois, M. Cosson, Biomechanical properties of vaginal tissue. part 1: new experimental protocol, J. Urol. 178 (1) (2007) 320–325.
[38] A.H. Lee, D.M. Elliott, Freezing does not alter multiscale tendon mechanics and damage mechanisms in tension, Ann. N.Y. Acad. Sci. 1409 (1) (2017) 85.
[39] M.L. Akins, K. Luby-Phelps, M. Mahendroo, Second harmonic generation imaging as a potential tool for staging pregnancy and predicting preterm birth, J. Biomed. Opt. 15 (2) (2010) 026020.
[40] K.R. Rosenberg, The evolution of modern human childbirth, Am. J. Phys. Anthropol. 35 (S15) (1992) 89–124.
[41] A. Feola, P.A. Moalli, M. Alperin, R. Duerr, R.E. Gandley, S.D. Abramowitch, Impact of pregnancy and vaginal delivery on the passive and active mechanics of the rat vagina, Ann. Biomed. Eng. 39 (1) (2011) 549–558.
[42] K.T. Downing, M. Billah, E. Raparia, A. Shah, M.C. Silverstein, A. Ahmad, G.S. Boutis, The role of mode of delivery on elastic fiber architecture and vaginal vault elasticity: a rodent model study, J. Mech. Behav. Biomed. Mater. 29 (2014) 190–198.
[43] A. Padoa, N.G. Fishman, A. Tsviban, N. Smorgick, Vaginal postcoital injuries requiring surgical intervention: a case series and literature review, Int. J. Impot. Res. (2020) 1–8.
[44] C. Deneux-Tharaux, E. Carmona, M.H. Bouvier-Colle, G. Bréart, Postpartum maternal mortality and cesarean delivery, Obstet. Gynecol. 108 (3) (2006) 541–548.